Contribution from the Department of Chemistry,
University of Missouri—Columbia, Columbia, Missouri 65211

Late-Transition-Metal μ-Oxo and μ-Imido Complexes. 6.[1] Gold(I) Imido Complexes

Visalakshi Ramamoorthy[†] and Paul R. Sharp*

Received January 24, 1990

The first group 11 imido complexes have been synthesized by two routes. Treating $[(LAu)_3O]BF_4$ (**1**) with excess RNH_2 gives $[(LAu)_3NR]BF_4$ (**2**) and H_2O (L = PPh_3, R = ^{t}Bu, Ph, *p*-FPh, *p*-BrPh, *p*-NO_2Ph). Alternatively, treating $[(LAu)_3O]BF_4$ with excess RNCO gives **2** and CO_2. A remarkable feature of the latter synthesis is the incorporation of ^{17}O into remaining PhNCO when $[(LAu)_3{}^{17}O]BF_4$ is used. Crystals of **2** (R = Ph) from CH_2Cl_2/ether are monoclinic ($C2/c$) with a = 22.103 (4) Å, b = 21.577 (9) Å, c = 25.85 (1) Å, β = 113.11 (3)°, V = 11336.6 Å^3, and Z = 8. The structure consists of well-separated cations and anions and half-occupancy CH_2Cl_2 of crystallization. The cationic portion shows three linear coordinate Au atoms with a μ_3-phenylimido nitrogen with a distorted tetrahedral geometry.

Introduction

We are investigating the synthesis and reaction chemistry of late-transition-metal oxo and imido complexes.[1] Our interest in these complexes is primarily as models for surface intermediates in reactions catalyzed by late-transition metals.[2] Among the complexes that we are studying is $[(LAu)_3O]^+BF_4$ (**1**) (L = PPh_3),[3] a potential model for oxygen adatoms on group 11 metal surfaces. Of particular interest is the observation that group 11 oxygen adatoms are capable of oxygen atom transfer to various substrates including alkenes.[4] We have found cases of formal oxygen atom transfer for **1** but also some unusual and surprising chemistry.[5] We are interested in extending this chemistry to the analogous imido complexes in hopes of finding examples of nitrene transfers and as an aid in understanding some of the more puzzling aspects of the chemistry of the oxo complex. To this end we have developed two synthetic routes to the first imido complexes of group 11.

Results

Syntheses. Suspensions of $[(LAu)_3O]BF_4$ (**1**) (L = PPh_3)[3] in THF rapidly dissolve when excess RNH_2 (R = Ph, *p*-FPh, *p*-BrPh, *p*-NO_2Ph, *t*-Bu) is added (eq 1). ^{31}P NMR spectra of the reaction

$$\underset{\mathbf{1}}{[(LAu)_3O]BF_4} + RNH_2 \rightarrow \underset{\mathbf{2}}{[(LAu)_3NR]BF_4} + H_2O \quad (1)$$

mixtures and the isolated products show only one peak between 28 and 29 ppm. The air-stable products, $[(LAu)_3NR]BF_4$ (**2**), are best isolated by precipitation with ether and may be recrystallized from THF/Et_2O (R = *t*-Bu) or CH_2Cl_2/Et_2O. The ^1H NMR spectrum of **2** (R = *t*-Bu) shows a singlet at 1.70 ppm and phenyl resonances at 7.4 ppm with an integrated ratio of 1:5. The $^{13}C\{^1H\}$ NMR spectrum has a singlet for the methyl carbons, a singlet for the tertiary carbon, and multiple signals for the phenyl carbons. The ^{17}O NMR spectrum of the reaction mixture has a single peak at 19.8 ppm. This peak is also observed in THF mixtures of $H_2{}^{17}O$ and *t*-$BuNH_2$ and presumably arises from an interaction of H_2O and *t*-$BuNH_2$. Curiously, we have found no indication that the reaction shown in eq 1 is reversible. The addition of excess H_2O to THF solutions of the imido complex **2** does not lead to precipitation of the oxo complex **1**. The ^{31}P NMR spectrum of the mixture is unchanged from that of **2** in the absence of added water. The signal does not shift nor does it broaden. If an equilibrium does exist, it must lie far to the right.

An alternative synthesis for **2** is shown in eq 2. All the same R groups work here. In the presence of 1 equiv of RNCO the

$$\underset{\mathbf{1}}{[(LAu)_3O]BF_4} + RNCO \rightarrow \underset{\mathbf{2}}{[(LAu)_3NR]BF_4} + CO_2 \quad (2)$$

reaction (in CH_2Cl_2) is very slow and decomposition products predominate over the formation of **2**. With excess RNCO the reaction is clean and rapid (minutes). The ^{17}O NMR spectrum of the reaction mixture (R = Ph) using ^{17}O-labeled **1** contains a single peak at 113 ppm. Surprisingly, this peak is not due to dissolved CO_2 (79 ppm[5,6]) but to remaining PhNCO,[7] which has become ^{17}O enriched (see Discussion).

Table I. Crystallographic Data for $[(LAu)_3NPh]BF_4 \cdot 0.5CH_2Cl_2$ (**2**·0.5CH_2Cl_2)

formula	$Au_3P_3F_4NC_{60}BH_{50} \cdot 0.5CH_2Cl_2$	space group	$C2/c$ (No. 15)
		T, °C	22
fw	1598.17	λ, Å	0.710 69
a, Å	22.103 (4)	d_{calc}, g·cm^{-3}	1.873
b, Å	21.577 (9)	μ(Mo Kα), cm^{-1}	79.14
c, Å	25.85 (1)	transm range, %	81.8-99.8
β, deg	113.11 (3)	$R(F_o)^a$	0.032
V, Å^3	11 336.6	$R_w(F_o)^b$	0.037
Z	8		

$^a R(F_o) = (\sum||F_o| - |F_c||)/\sum F_o$. $^b R_w(F_o) = [(\sum w(|F_o| - |F_c|)^2)/\sum wF_o^2]^{1/2}$; $w = 4F_o^2/(\sigma(F_o)^2)^2$; p = 0.04.

Solid-State Structure of 2 (R = Ph). Crystals of **2** suitable for X-ray analysis were readily obtained for R = Ph. An ORTEP view of the structure is given in Figure 1. An abbreviated listing of crystallographic and data collection parameters is given in Table I (a full table is given in the supplementary material), positional parameters are given in Table II, and selected interatomic distances and angles are given in Table III.

The structure consists of isolated cations and anions with a highly disordered methylene chloride of crystallization (ca. $^1/_2$ occupancy). The overall geometry of the cationic portion is very similar to that found for the parent oxo complex **1**[3] and the nitride $[(LAu)_4N]^+$.[8] The oxo complex **1**, however, is unique in that a dimerization via two Au-Au interactions occurs to form a dimeric arrangement of the trinuclear cations.[3] The absence of this interaction in **2** and the nitride is presumably due to steric constraints imposed by the imido phenyl ring and the fourth AuL group. The intracationic Au-Au distances in **2** show a larger variation than in **1** but a smaller variation than in the nitride. The smallest is very short at 2.926 (1) Å, leading to a small Au-N-Au angle of 89.4 (3)°. The next is only slightly longer at 3.014 (1) Å with a Au-N-Au angle of 94.2 (3)°, and the longest is 3.333 (1) Å with a Au-N-Au angle of 108.1 (4)°. As a result of these interactions and the small Au-N-Au angles, the remaining angles around the nitrogen involving the phenyl ring carbon C1 are all

[†] Permanent address: Bhabha Atomic Research Center, Trombay, Bombay 400-085, India.

(1) Part 5: Ge, Y.-W.; Sharp, P. R. *J. Am. Chem. Soc.* **1990**, *112*, 3667-3668.
(2) (a) Madix, R. J.; Jorgensen, S. W. *Surf. Sci.* **1987**, *183*, 27-43. (b) Akhter, S.; White, J. M. *Surf. Sci.* **1986**, *167*, 101-126. (c) Berlowitz, P.; Yang, B. L.; Butt, J. B.; Kung, H. H. *Surf. Sci.* **1986**, *171*, 69-82. (d) Outka, D. A.; Madix, R. J. *J. Am. Chem. Soc.* **1987**, *109*, 1708-1714 and references cited therein.
(3) Nesmeyanov, A. N.; Perevalova, E. G.; Struchkov, Yu. T.; Antipin, M. Yu.; Grandberg, K. I.; Dyadchenko, V. P. *J. Organomet. Chem.* **1980**, *201*, 343.
(4) Roberts, J. T.; Madix, R. J. *J. Am. Chem. Soc.* **1988**, *110*, 8540-8541.
(5) Visalakshi, R.; Sharp, P. R. Manuscript in preparation.
(6) Wasylishen, R. E.; Mooibroek, S.; Macdonald, J. B. *J. Chem. Phys.* **1984**, *81*, 1057-1059.
(7) Boykin, D. W. *Spectrosc. Lett.* **1987**, *20*, 415-422.
(8) Slovokhotov, Y. L.; Struchkov, Y. T. *J. Organomet. Chem.* **1984**, *277*, 143-146.

0020-1669/90/1329-3336$02.50/0

Table II. Refined Positional Parameters for $[(LAu)_3NPh]BF_4 \cdot 0.5CH_2Cl_2$ ($2 \cdot CH_2Cl_2$)

atom[a]	x	y	z	B, Å²[b]	atom[a]	x	y	z	B, Å²[b]
Au1	0.08679 (2)	0.10856 (2)	0.06351 (2)	3.42 (1)	C46	0.3441 (9)	0.1705 (7)	0.2207 (5)	8.9 (5)
Au2	0.21904 (2)	0.08119 (2)	0.06043 (2)	3.52 (1)	C51	0.3887 (5)	0.0813 (6)	0.1127 (5)	5.1 (3)
Au3	0.15418 (2)	−0.03167 (2)	0.07524 (2)	3.40 (1)	C52	0.3877 (6)	0.0562 (6)	0.0630 (5)	5.9 (4)
P1	0.0523 (1)	0.1808 (1)	0.1081 (1)	3.91 (8)	C53	0.4450 (6)	0.0291 (7)	0.0627 (6)	7.7 (4)
P2	0.3174 (1)	0.1215 (2)	0.1126 (1)	4.24 (8)	C54	0.5033 (6)	0.0281 (9)	0.1096 (7)	9.6 (5)
P3	0.1997 (1)	−0.1113 (1)	0.1331 (1)	3.95 (8)	C55	0.5034 (7)	0.050 (1)	0.1586 (7)	11.0 (6)
N	0.1238 (4)	0.0464 (4)	0.0243 (3)	3.3 (2)	C56	0.4458 (6)	0.0772 (9)	0.1597 (6)	9.4 (5)
C1	0.0917 (5)	0.0362 (5)	−0.0345 (4)	3.2 (3)	C61	0.3243 (5)	0.2029 (6)	0.0944 (4)	5.3 (3)
C2	0.1264 (5)	0.0182 (5)	−0.0666 (5)	4.7 (3)	C62	0.2706 (7)	0.2394 (6)	0.0799 (5)	6.5 (4)
C3	0.0953 (6)	0.0070 (6)	−0.1236 (5)	6.0 (4)	C63	0.2737 (8)	0.3031 (7)	0.0652 (6)	8.7 (5)
C4	0.0272 (6)	0.0145 (6)	−0.1499 (4)	6.1 (4)	C64	0.3362 (8)	0.3222 (8)	0.0706 (6)	11.9 (5)
C5	−0.0088 (6)	0.0300 (6)	−0.1180 (5)	5.8 (4)	C65	0.3868 (9)	0.2908 (9)	0.0827 (8)	14.3 (6)
C6	0.0229 (5)	0.0405 (5)	−0.0607 (4)	4.3 (3)	C66	0.3817 (7)	0.2258 (7)	0.0960 (6)	8.7 (5)
C11	0.0788 (5)	0.2585 (5)	0.1009 (5)	4.6 (3)	C71	0.1952 (5)	−0.1061 (5)	0.2015 (4)	4.3 (3)
C12	0.0951 (9)	0.3009 (7)	0.1426 (6)	9.5 (6)	C72	0.1904 (6)	−0.0485 (6)	0.2213 (4)	5.4 (3)
C13	0.113 (1)	0.3618 (8)	0.1322 (8)	12.4 (8)	C73	0.1926 (7)	−0.0429 (7)	0.2762 (6)	7.4 (4)
C14	0.1126 (8)	0.3780 (7)	0.0836 (7)	9.4 (5)	C74	0.1989 (8)	−0.0952 (7)	0.3097 (5)	8.7 (5)
C15	0.098 (1)	0.3359 (8)	0.0447 (8)	13.9 (7)	C75	0.2028 (8)	−0.1503 (8)	0.2878 (5)	9.5 (5)
C16	0.0858 (9)	0.2741 (7)	0.0535 (7)	10.5 (6)	C76	0.2017 (7)	−0.1569 (6)	0.2349 (5)	7.4 (4)
C21	0.0829 (5)	0.1676 (6)	0.1838 (4)	4.8 (3)	C81	0.1681 (5)	−0.1870 (5)	0.1081 (4)	4.0 (3)
C22	0.1522 (9)	0.163 (1)	0.2150 (8)	6.3 (5)*	C82	0.2055 (6)	−0.2357 (5)	0.1069 (5)	5.5 (3)
C22′	0.132 (1)	0.133 (1)	0.209 (1)	3.7 (7)*	C83	0.1792 (6)	−0.2931 (6)	0.0884 (5)	6.9 (4)
C23	0.175 (1)	0.152 (1)	0.2729 (9)	7.0 (5)*	C84	0.1145 (7)	−0.3020 (6)	0.0699 (5)	7.0 (4)
C23′	0.157 (2)	0.126 (2)	0.271 (1)	5.8 (9)*	C85	0.0747 (8)	−0.2538 (7)	0.0712 (7)	8.9 (5)
C24	0.132 (1)	0.138 (1)	0.2987 (9)	7.3 (6)*	C86	0.1024 (7)	−0.1949 (6)	0.0895 (6)	6.9 (4)
C24′	0.138 (2)	0.175 (2)	0.301 (1)	5.3 (8)*	C91	0.2868 (5)	−0.1142 (6)	0.1468 (4)	4.7 (3)
C25	0.071 (1)	0.126 (2)	0.268 (1)	12 (1)*	C92	0.3340 (7)	−0.129 (1)	0.1986 (7)	11.4 (6)
C25′	0.089 (2)	0.211 (2)	0.276 (1)	5.6 (9)*	C93	0.4010 (7)	−0.127 (1)	0.2069 (7)	13.1 (7)
C26	0.040 (1)	0.143 (1)	0.206 (1)	9.5 (7)*	C94	0.4163 (7)	−0.1117 (9)	0.1619 (7)	10.5 (6)
C26′	0.057 (1)	0.208 (1)	0.214 (1)	4.3 (7)*	C95	0.3713 (6)	−0.0957 (6)	0.1129 (6)	6.7 (4)
C31	−0.0364 (5)	0.1872 (5)	0.0829 (4)	3.4 (3)	C96	0.3068 (5)	−0.0966 (5)	0.1057 (5)	5.0 (3)
C32	−0.0727 (5)	0.1351 (5)	0.0638 (5)	4.9 (3)	B	0.2016 (7)	0.4644 (7)	0.5689 (6)	5.6 (4)
C33	−0.1409 (6)	0.1368 (6)	0.0440 (5)	5.6 (4)	F1	0.2205 (4)	0.5247 (4)	0.5648 (3)	7.6 (2)
C34	−0.1718 (6)	0.1916 (6)	0.0438 (5)	6.0 (4)	F2	0.1448 (4)	0.4624 (4)	0.5723 (4)	11.9 (3)
C35	−0.1347 (6)	0.2438 (6)	0.0625 (6)	7.0 (4)	F3	0.2511 (4)	0.4383 (4)	0.6156 (4)	10.0 (3)
C36	−0.0679 (6)	0.2411 (6)	0.0812 (6)	6.6 (4)	F4	0.2025 (5)	0.4319 (4)	0.5251 (4)	11.5 (3)
C41	0.3265 (5)	0.1208 (5)	0.1851 (5)	4.5 (3)	CS	−0.975 (1)	0.839 (1)	0.272 (1)	0.56[c]
C42	0.3156 (6)	0.0674 (7)	0.2067 (5)	6.8 (4)	Cl1	−1.0345 (9)	0.809 (1)	0.2965 (8)	0.22[c]
C43	0.3210 (6)	0.0608 (7)	0.2623 (6)	7.4 (4)	Cl2	−1.0222 (7)	0.7661 (8)	0.2779 (6)	0.27[c]
C44	0.3400 (7)	0.1113 (7)	0.2958 (5)	7.9 (4)	Cl3	−1.038 (1)	0.846 (1)	0.2657 (8)	0.21[c]
C45	0.3521 (9)	0.1652 (8)	0.2764 (6)	10.9 (6)					

[a] Primed atoms represent the minor (35%) second orientation for phenyl ring 2. [b] Thermal parameters are given in the form of the isotropic equivalent displacement parameter defined as $(4/3)[a^2\beta(1,1) + b^2\beta[2,2) + c^2\beta(3,3) + ab(\cos\gamma)\beta(1,2) + ac(\cos\beta)\beta(1,3) + bc(\cos\alpha)\beta(2,3)$. Starred values indicate atoms were refined isotropically. [c] Solvent occupancy values with fixed $\beta = 9.0°$.

Table III. Selected Intramolecular Distances (Å) and Angles (deg) for **2** (R = Ph)

Au1-Au2	3.014 (1)	Au2-N	2.079 (7)
Au1-Au3	3.333 (1)	N-C1	1.42 (1)
Au2-Au3	2.926 (1)	C1-C2	1.39 (2)
Au1-P1	2.242 (3)	C2-C3	1.38 (2)
Au3-P3	2.240 (3)	C3-C4	1.40 (2)
Au2-P2	2.237 (3)	C4-C5	1.39 (2)
Au1-N	2.035 (9)	C5-C6	1.38 (1)
Au3-N	2.080 (8)	C6-C1	1.40 (1)
P1-Au1-N	176.1 (3)	N-C1-C2	121.4 (9)
P2-Au2-N	169.9 (3)	N-C1-C6	120 (1)
P3-Au3-N	172.9 (3)	C2-C1-C6	118.5 (8)
Au1-N-Au2	94.2 (3)	C1-C2-C3	122 (1)
Au1-N-Au3	108.2 (3)	C2-C3-C4	119 (1)
Au1-N-C1	120.3 (6)	C3-C4-C5	119.9 (9)
Au2-N-Au3	89.4 (2)	C4-C5-C6	120 (1)
Au2-N-C1	122.0 (8)	C1-C6-C5	120 (1)
Au3-N-C1	117.0 (6)		

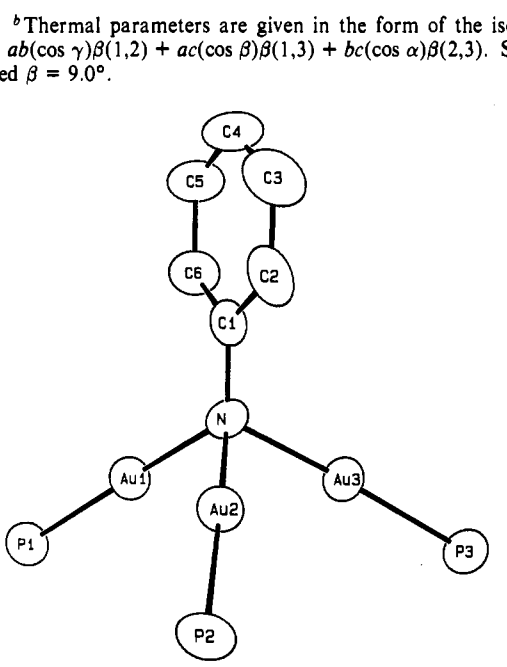

Figure 1. ORTEP view of the cationic portion of $[(LAu)_3NR]BF_4$ (**2**) (L = PPh_3, R = Ph) with 50% probability ellipsoids. Phosphine phenyl rings are omitted for clarity.

large and range from 117 to 122°. The three Au–N distances are somewhat smaller than the sum of covalent radii (2.12 Å) and are divided into one short (2.035 (9) Å) and two longer equal distances (2.080 (8) and 2.079 (7) Å). The two longer distances are to the Au atoms that have the shortest Au–Au distance. The nitride also shows a range of Au–N distances (1.93 (2)–2.10 (2) Å), the average of which (2.01 Å) is somewhat smaller than that of **2** (2.06 Å). The average Au–O distance in **1** is 1.97 (4) Å, equivalent within the standard deviations to the Au–N distances in **2** and the nitride even before correction for the ca. 0.02 Å greater covalent radius of N. The Au–P distances of **2** are typical and show little variation. The coordination geometry about the Au atoms is nearly linear with P–Au–N angles of 169.9 (3), 172.8

Scheme I

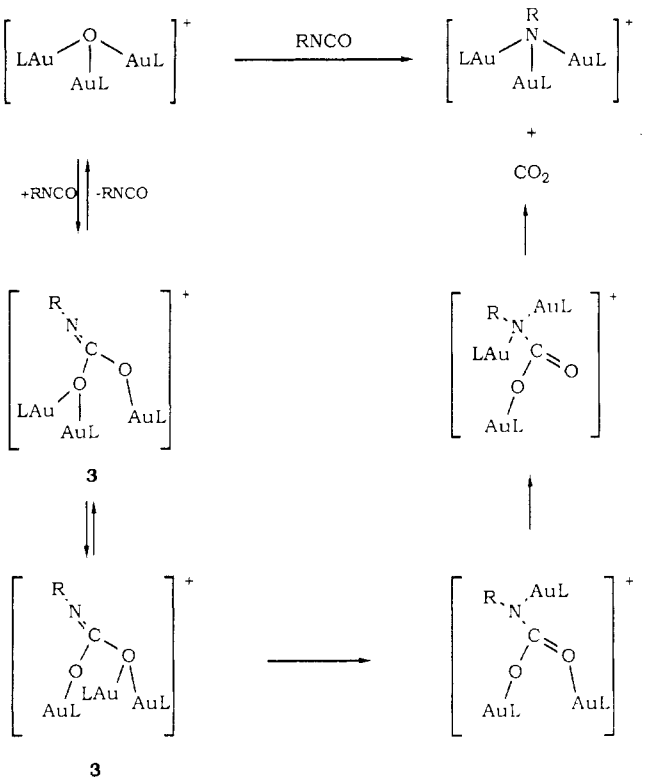

(2), and 176.1 (2)°. The two with the greatest deviation from linearity (Au3 and Au2) are the ones involved in the shortest Au–Au interaction.

Discussion

The two syntheses of the imido complexes **2** follow well-established methods commonly applied to terminal-early-transition-metal oxo complexes.[9,10] Our results and those of others[11] suggest that these methods also work well for late-transition-metal μ-oxo complexes and can be applied to the preparation of a wide range of substituted late-transition-metal μ-imido complexes.

A remarkable feature of the isocyanate synthesis (eq 2) is the observation of ^{17}O incorporation into the excess phenyl isocyanate. This indicates a reversible interaction of the isocyanate with the oxo complex **1**. This can occur either if the reaction is totally reversible or if there is a rapid and reversible preequilibrium step, which exchanges the oxo and isocyanate oxygens, prior to an irreversible step. A proposed pathway for the reaction is given in Scheme I. The key species **3** leading to the oxygen exchange is a metallocarbamate complex. Monometallic cyclic analogues have been characterized[12] including one from the reaction of a Mo oxo complex and PhNCO.[13] Both a totally reversible reaction and a rapid preequilibrium can be fitted to the scheme. For either case, the reactions leading to **3** would have to be reversible. Coordination of all three LAu^+ fragments is included in the scheme. This may or may not be the case. Indeed, the decomposition observed in the absence of excess isocyanate suggests that uptake of an LAu^+ fragment by a second RNCO may be required for the reaction to go cleanly.

Finally, a correlation between the ^{13}C NMR data of multiply bonded *t*-Bu imido complexes and the electron density on the imido nitrogen has been noted.[9,14] The difference (Δ) between the chemical shifts of the α- and β-carbons is used. Smaller Δ values indicate increasing electron density. If this correlation holds for the *t*-Bu Au imido complex **2**, then the Δ value of 21 would suggest electron density on the nitrogen nearly equal to that in Ph_3PN-(*t*-Bu) (Δ = 16). This seems inconsistent with the positive charge of **2**; however, the removal of an LAu^+ fragment does generate a highly basic complex.[5]

Experimental Section

Materials and Methods. All the reactions were performed under a dry nitrogen atmosphere by using normal Schlenk techniques and a Vacuum Atmospheres glovebox equipped with an HE-493 Dri-Train. Tetrahydrofuran (THF) and ether were dried over sodium benzophenone ketyl and distilled prior to use. Methylene chloride was distilled from P_2O_5. Amines were distilled from CaH_2. $AuPPh_3Cl$[15] and **1**[3] were prepared according to reported methods. Infrared spectra (4000–600 cm^{-1}) were recorded on a Nicolet 20-DXB spectrometer as thin films or mineral oil mulls on NaCl plates.

$^{31}P\{^1H\}$ NMR spectra were recorded at ambient temperature on NICOLET NT-300 or JEOL FX-90 spectrometer operating in the Fourier transform mode. ^{31}P chemical shifts are referenced to external H_3PO_4. $^{17}O\{^1H\}$ NMR spectra were obtained on the Nicolet spectrometer (40.7 MHz) with a 5-mm probe and are referenced to external water (0 ppm). ^{17}O-enriched **1**[5] was used for all ^{17}O NMR measurements. Elemental analysis were performed by Oneida Research Services, Whitesboro, NY.

Preparation of $[(AuPPh_3)_3NR]BF_4$ (2). The preparations for all R groups are similar, giving yields between 70 and 95%. Representative syntheses are given below. All complexes are white except for **2** (R = *p*-NO_2Ph), which is yellow. The $^{31}P\{^1H\}$ NMR (36 MHz, CD_2Cl_2) spectra of the phenyl-substituted complexes are essentially identical and consist of single sharp peaks at 28.3 (1) ppm. Melting point and IR data and a microanalysis for **2** (R = *p*-NO_2Ph) are included as supplementary material.

A. From RNH_2. Preparation of $[(AuPPh_3)_3NBu^t]BF_4$ (2). *tert*-Butylamine (0.30 mL, 2.9 mmol) was added to a stirred suspension of **1** (0.80 g, 0.54 mmol) in THF (20 mL). After 15 min a homogeneous solution formed. Stirring was continued for 1 h. The solution was then concentrated in vacuo to 5 mL, and 50 mL of ether was added. The white precipitate was removed by filtration and dried in vacuo. Recrystallization was achieved by dissolving the product in a minimum volume of THF, adding an equal volume of Et_2O, and cooling at −20 °C overnight. The white crystalline product was removed by filtration and dried. Yield: 0.70 g (80%). Anal. Calcd (found) for $C_{58}H_{54}Au_3BF_4NP_3$: C 45.36 (46.3); H, 3.54 (3.5); N, 0.91 (0.6). ^1H NMR (90 MHz, CD_2Cl_2), δ: 7.3–7.5 (m, 45 H, Ph), 1.70 (s, 9 H, *t*-Bu). $^{13}C\{^1H\}$ NMR (22.5 MHz, CD_2Cl_2), δ: 134.6, 133.9, 132.1, 129.8, 129.3 (Ph); 65.1 (CMe_3); 43.7 ($C(CH_3)_3$). $^{31}P\{^1H\}$ NMR (36 MHz, CD_2Cl_2), δ: 29.0.

B. From RNCO. Preparation of $[(AuPPh_3)_3NPh]BF_4$. PhNCO (0.20 mL, 1.8 mmol) in CH_2Cl_2 (0.4 mL) was added dropwise to a stirred solution of **1** (0.106 g, 0.072 mmol) in CH_2Cl_2 (0.5 mL). After 24 h the volatiles were removed in vacuo from the yellow solution. The residue was washed with *n*-hexane and dissolved in a minimum volume of CH_2Cl_2. Ether was added, and the mixture was cooled at −20 °C overnight. The resulting light brown crystals were removed by filtration and dried in vacuo. Yield: 90 mg (81%). Anal. Calcd (found) for $C_{60}H_{51}Au_3BF_4NP_3$: C, 45.47 (45.5); H, 3.22 (3.2); N, 0.88 (0.8).

Structure Analyses. An abbreviated summary of crystallographic data is given in Table I. Crystals of **2** (R = Ph) were grown as described above. A crystal was selected and mounted on the end of a glass fiber in air. Cell dimensions were based upon a Delaunay reduction of a cell obtained from the centering of 25 reflections on the diffractometer (Enraf-Nonius CAD4). Intensity data were measured with MoKα radiation from a graphite monochronomator (θ–2θ scan, 96 steps/scan, 16 steps/side background). The intensities of three standard reflections were measured after each 7200-s exposure to the X-rays and showed no decay of intensity during the course of the experiment. An empirical absorption correction was applied based on Ψ scans. The Enraf-Nonius SDP program package was used for all calculations. The structure was resolved by

(9) For a review see: Nugent, W. A.; Haymore, B. L. *Coord. Chem. Rev.* **1980**, *31*, 123.
(10) (a) Horton, A. D.; Schrock, R. R.; Freudenberger, J. H. *Organometallics* **1987**, *6*, 893. (b) Green, M. H. L.; Moynihan, K. J. *Polyhedron* **1986**, *5*, 921. (c) Maatta, E. A. *Inorg. Chem.* **1984**, *23*, 2560. (d) Bradley, D. C.; Hursthouse, M. B.; Malik, K. M. A.; Nielson, A. J.; Short, R. L. *J. Chem. Soc., Dalton Trans.* **1983**, 2651. (e) Schrock, R. R.; Pedersen, S. F. *J. Am. Chem. Soc.* **1982**, *104*, 7483. (f) Chen, G. J.-J.; McDonald, J. W.; Newton, W. E. *Inorg. Chim. Acta* **1980**, *41*, 49.
(11) McGhee, W. D.; Foo, T.; Hollander, F. J.; Bergman, R. G. *J. Am. Chem. Soc.* **1988**, *110*, 8543–8545.
(12) Glueck, D. S.; Hollander, F. J.; Bergman, R. G. *J. Am. Chem. Soc.* **1989**, *111*, 2719–2721.
(13) Jernakoff, P.; Geoffroy, G. L.; Rheingold, A. L.; Geib, S. J. *J. Chem. Soc., Chem. Commun.* **1987**, 1610–1611.
(14) Nugent, W. A.; McKinney, R. J.; Kasowski, R. V.; Van-Catledge, F. A. *Inorg. Chim. Acta* **1982**, *65*, L91–L93.
(15) Kowala, C.; Swan, J. M. *Aust. J. Chem.* **1966**, *19*, 547–554.

direct methods followed by successive applications of Fourier methods. Phenyl hydrogen atoms were placed in calculated fixed positions. Full-matrix least-squares refinement minimizing $\sum w(|F_o| - |F_c|)^2$ converged to the R values given in Table I. No extinction correction was applied. A disordered CH_2Cl_2 molecule, well separated from the anionic and cationic portions, was included. Final atomic positional parameters for the refined atoms are included in Table II. Selected bond distances and angles are given in Table III. Other data are included as supplementary material.

Acknowledgment. We thank ARCO Chemical Co. and the Division of Chemical Sciences, Office of Basic Energy Sciences, Office of Energy Research, U.S. Department of Energy (Contract DE-FG02-88ER13880), for support of this work. The National Science Foundation provided a portion of the funds for the purchase of the X-ray (Grant CHE-7820347) and NMR (Grant PCM-8115599) equipment.

Supplementary Material Available: Tables of melting point and IR data, full crystallographic data and data collection parameters, fractional coordinates, thermal parameters, and additional distances and angles (6 pages); a listing of structure factors (25 pages). Ordering information is given on any current masthead page.

Contribution from the Department of Chemistry, The University of Alberta, Edmonton, Alberta, Canada T6G 2G2

Ascertaining the Roles of Each Metal in the Activation of S-H Bonds in Hydrogen Sulfide and Thiols by the Heterobinuclear Complex $[RhRe(CO)_4(Ph_2PCH_2PPh_2)_2]$

David M. Antonelli and Martin Cowie*

Received December 11, 1989

The reactions of H_2S, HSEt, and HSPh with $[RhRe(CO)_4(dppm)_2]$ have been studied. These reactions are facile at ambient temperature, yielding $[RhRe(CO)_4(\mu\text{-}S)(dppm)_2]$ (**2**) in the case of H_2S and $[RhRe(CO)_3(\mu\text{-}H)(\mu\text{-}SR)(dppm)_2]$ (R = Et (**5**) Ph (**6**)) for the thiols. Monitoring these reactions at −80 °C by ^{31}P, ^{13}C, and ^1H NMR spectroscopy indicates that in all cases the first species is the HSR adduct (R = H, Et, Ph), which then yields $[RhRe(CO)_4(SR)(\mu\text{-}H)(dppm)_2]$ via oxidative addition of an S-H bond. In subsequent steps the reactions involving H_2S and thiols proceed differently. In the case of H_2S, the presumed second S-H oxidative addition step is followed by facile H_2 loss, and no additional intermediate is observed before formation of **2**, even at −60 °C. For ethanethiol no other intermediate is observed before formation of **5**; however, for benzenethiol a tetracarbonyl species, in which the hydride ligand has migrated to Re, is observed after the hydride-bridged species, followed by movement of the thiolate group to the bridging position with concomitant loss of one carbonyl to give **6**. Mechanisms for these transformations are proposed. The structure of **5** was determined by X-ray techniques, confirming that the thiolate group and the hydride ligand bridge the metals on opposite faces of the dimer. Compound **5** crystallizes in the monoclinic space group $P2_1/c$ with a = 12.216 (3) Å, b = 19.845 (7) Å, c = 23.316 (7) Å, β = 103.19 (2) Å, V = 5503 Å^3, and Z = 4 and has refined to R = 0.049 and R_w = 0.056 on the basis of 370 parameters varied and 5011 independent observations.

Introduction

The current interest in binuclear complexes is based on the assumption that the presence of the two adjacent metals will give rise to reactivity patterns that differ substantially from those of the mononuclear analogues. With this idea in mind, we have chosen to investigate chemistry that might clearly benefit from the presence of two adjacent metals, and as part of this study, we have been examining the activation of adjacent heteroatom-hydrogen bonds in H_2X molecules (X = S, Se, SiR_2, SiHR).[1,2] We are interested in the initial sites of substrate attack in various binuclear complexes, the involvement of the adjacent metals in X-H bond activation processes, the chemically significant ligand rearrangements that occur, and the possibility of subsequent binuclear reductive elimination reactions. In this paper we present details about the activation of H_2S and thiols. Hydrogen sulfide is of interest to us because of its potential use as a source of H_2[3-6] and organosulfur compounds,[7] whereas thiols may serve to model unstable intermediates both in the initial S-H activation processes involving H_2S and in the subsequent formation of organosulfur products.

Although our initial studies involved homo- and heterobinuclear complexes of Rh and Ir,[1,2] we have recently turned to heterobinuclear complexes in which Rh is combined with an earlier transition metal.[8] The compound of interest in this study, $[RhRe(CO)_4(dppm)_2]$ (**1**) (dppm = $Ph_2PCH_2PPh_2$), has the

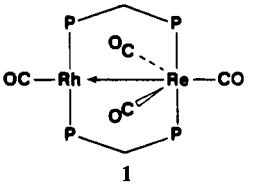

1

structure shown, in which a dative bond between the coordinatively saturated Re(−1) center and the unsaturated Rh(+1) center can be formulated.[8] Consistent with the coordinative unsaturation at Rh and the low oxidation states of the metals, compound **1** has been found to be active toward oxidative addition reactions, involving substrates such as H_2, Cl_2, and HCl,[9] and so seemed a good candidate for oxidative addition reactions of H-S bonds in H_2S and thiols. It was hoped that the strong tendency of Re to maintain an 18-electron configuration might allow the characterization of intermediates that were difficult to observe when the second metal was Rh or Ir.[1,2]

In a related study involving the reaction of H_2S with $[Pd_2Cl_2(dppm)_2]$,[3] activation of both H-S bonds followed by facile

(1) McDonald, R.; Cowie, M. *Organometallics*, in press.
(2) McDonald, R.; Cowie, M. Manuscript in preparation.
(3) (a) Lee, C-L.; Besenyei, G.; James, B. R.; Nelson, D. A.; Lilga, M. A. *J. Chem. Soc., Chem. Commun.* **1985**, 1175. (b) Besenyei, G.; Lee, C.-L.; Gulinski, J.; Rettig, S. J.; James, B. R.; Nelson, D. A.; Lilga, M. A. *Inorg. Chem.* **1987**, *26*, 3622. (c) Lee, C.-L.; Chisholm, J.; James, B. R.; Nelson, D. A.; Lilga, M. A. *Inorg. Chim. Acta* **1986**, *121*, L7.
(4) Mueting, A. M.; Boyle, P.; Pignolet, L. H. *Inorg. Chem.* **1984**, *23*, 44.
(5) Bianchini, C.; Mealli, C.; Meli, A.; Sabat, M. *Inorg. Chem.* **1986**, *25*, 4617.
(6) Bottomley, F.; Drummond, D. F.; Egharevba, G. O.; White, P. S. *Organometallics* **1986**, *5*, 1620.
(7) Mueting, A. M.; Boyle, P. D.; Wagner, R.; Pignolet, L. H. *Inorg. Chem.* **1988**, *27*, 271 and references therein.
(8) Antonelli, D. M.; Cowie, M. *Organometallics* **1990**, *9*, 1818.
(9) Antonelli, D. M.; Cowie, M. *Organometallics*, in press.

0020-1669/90/1329-3339$02.50/0